Title
Changes in hydrogen production and polymer accumulation upon sulfur-deprivation in purple photosynthetic bacteria

Journal
International Journal of Hydrogen Energy, 34(15)

ISSN
0360-3199

Authors
Melnicki, Matthew R
Eroglu, Ela
Melis, Anastasios

Publication Date
2009-08-01

DOI
10.1016/j.ijhydene.2009.05.115

Peer reviewed

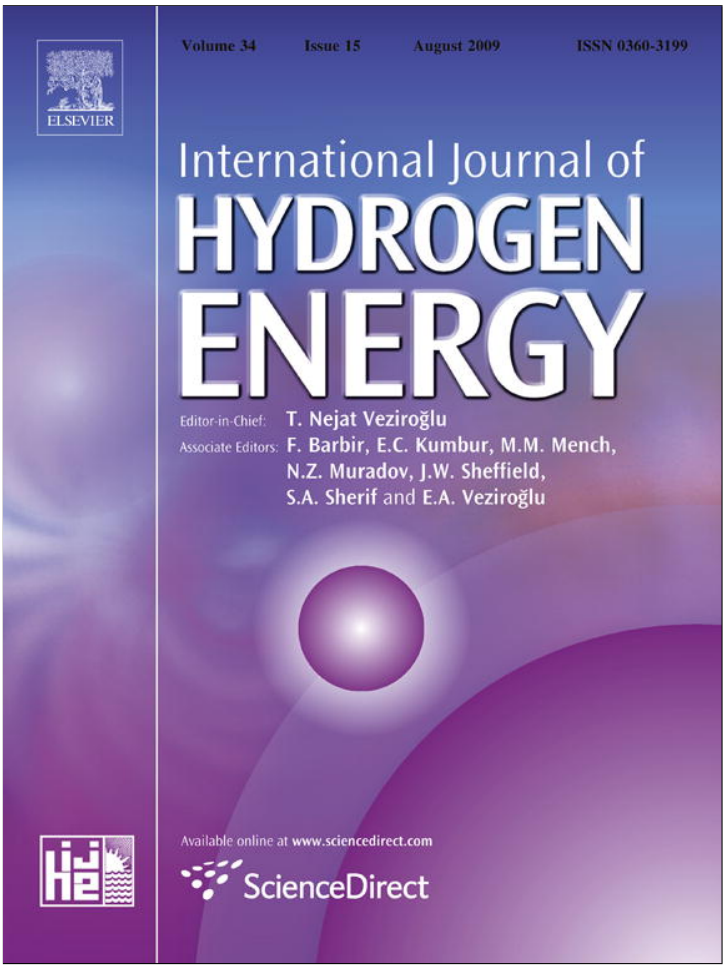

INTERNATIONAL JOURNAL OF HYDROGEN ENERGY 34 (2009) 6157–6170

Available at www.sciencedirect.com

ScienceDirect

journal homepage: www.elsevier.com/locate/he

Changes in hydrogen production and polymer accumulation upon sulfur-deprivation in purple photosynthetic bacteria

Matthew R. Melnicki[a], *Ela Eroglu*[b], *Anastasios Melis*[a,b,*]

[a]*Agricultural & Environmental Chemistry, University of California, 111 Koshland Hall, MC-3102, Berkeley, CA 94720, USA*
[b]*Plant & Microbial Biology, University of California, Berkeley, CA 94720-3102, USA*

ARTICLE INFO

Article history:
Received 19 March 2009
Received in revised form
27 May 2009
Accepted 28 May 2009
Available online 25 June 2009

Keywords:
Hydrogen production
Purple photosynthetic bacteria
Rhodospirillum rubrum
Rhodopseudomonas palustris
Rhodobacter sphaeroides
Nitrogenase
Sulfur-deprivation
Poly-β-hydroxybutyrate

ABSTRACT

The work investigated physiological conditions directing cellular metabolism toward either H_2-production or storage polymer accumulation in purple photosynthetic bacteria. Hydrogen-producing cultures of the purple anoxygenic photosynthetic bacterium *Rhodospirillum rubrum* were resuspended in media lacking sulfur (S) nutrients. S-deprived cultures displayed lack of growth, cessation of bacteriochlorophyll and protein accumulation, and inhibition of H_2 evolution. Cell volume increased substantially and large amounts of polymer were found to accumulate extracellularly. Poly-β-hydroxybutyrate (PHB) content increased about 3.5-fold within 24 h of S-deprivation. Most cells remained viable after 100 h of S-deprivation and cultures were capable of resuming growth and H_2-production when supplemented with sulfate. Transcript levels, protein amount, and activity of the nitrogenase enzyme, which are responsible for H_2-production, decreased with a halftime of about 15 h upon S-deprivation. In addition, the nitrogenase NifH subunits were modified by ADP-ribosylation, indicating post-translational inactivation. Comparative aconitase activity measurements of control and S-deprived cells failed to indicate a general stress to Fe–S proteins, as aconitase, a Fe–S protein in the citric acid cycle sensitive to oxidative stress, maintained activity throughout the course of the S-deprivation. In contrast to *nifH* transcriptional down-regulation, expression of *cysK* (encoding cysteine synthase) was upregulated in response to S-deprivation. The described physiology is not specific to *R. rubrum*, as *Rhodobacter sphaeroides* and *Rhodopseudomonas palustris* exhibited a similar response to S-deprivation. It is suggested that manipulation of the supply of S-nutrients may serve as a tool for the alternative production of H_2 or PHB in purple photosynthetic bacteria, thus affording opportunities to design photobiological systems that serve in both energy conversion and storage processes.

1. Introduction

Purple photosynthetic bacteria are versatile microorganisms that can utilize energy from sunlight to drive metabolism, cellular growth and catalysis [1]. Among the biochemical processes linked to purple bacterial photosynthesis are a number of enzymatic conversions that may yield economically valuable products such as biofuels and biopolymers [2,3].

Abbreviations: BChl, bacteriochlorophyll; PHB, poly-β-hydroxybutyrate; SMN, supplemented minimal medium; DIC, differential interference contrast; FITC, fluorescein isothiocyanate; dsRed, *Discosoma* sp. red fluorescent protein; PCV, packed cell volume.

* *Corresponding author*. Fax: +1 510 642 4995.
E-mail address: melis@nature.berkeley.edu (A. Melis).

0360-3199/$ – see front matter
doi:10.1016/j.ijhydene.2009.05.115

Hydrogen is one such industrial product that may be derived from purple bacteria, with the enzyme nitrogenase [4] utilizing photosynthetically-derived ATP and electrons for the reduction of protons to molecular hydrogen (H_2) [5]. Unlike unicellular green algae, which produce H_2 from electrons derived from oxygenic photosynthesis [6], purple bacteria are capable of producing H_2 continuously with energy from sunlight, on account of their anoxygenic form of photosynthesis, leading to much higher yields than currently achieved with green algae. Purple bacteria additionally possess the ability to fix N_2 into organic sources of nitrogen (e.g. NH_3 for fertilizer), to biosynthesize storage polymers, and to utilize wavelengths of sunlight that are complementary to those used by oxygenic photosynthetic organisms [7]. Thus, purple bacteria can serve as attractive catalysts for the generation of high value bio-products.

However, purple bacteria require an exogenous electron-donating substrate, such as small organic acids (i.e., succinate), in order to operate photosynthesis, whereas oxygenic phototrophs, such as green algae, can use abundant H_2O molecules as substrate. While these small organic acid compounds are not as expensive as sugars, which serve as the substrate for dark, fermentative hydrogen production [8], they still present an added cost for the photosynthetic production of hydrogen. Thus, improvements in the yield of H_2-production are needed to enhance prospects of purple bacterial commercialization [9–13]. One strategy is to reduce the cost of the electron-donating substrate by utilizing industrial wastewaters that otherwise need to be disposed [14,15]. Alternatively, value may be enhanced via optimization of the substrate partitioning between cellular biomass and product generation. This may be accomplished through improving the molar yield efficiency of hydrogen production [16,17], or by co-generating additional valuable compounds [18].

Research effort over the past decade has been carried out to advance the field of photobiological H_2-production by unicellular green algae [6]. Sulfur nutrient deprivation of unicellular green microalgae was used as a tool in altering cellular metabolism, thus redirecting photosynthetic electron transport toward hydrogen production [19,20]. The premise of this approach is that a lack of S-nutrients prevents *de novo* biosynthesis of the S-containing amino acids cysteine and methionine [21], thereby inhibiting protein accumulation and organismal growth. Under these conditions, green microalgae direct cellular metabolism toward starch accumulation [12,22], while inducing an alternative pathway of electron transport in their chloroplast, whereby photosynthetic electrons and protons are catalytically converted into H_2 by the enzyme [Fe]-hydrogenase. The process of H_2-production under anaerobic conditions serves to maintain redox poise in the green microalgae and to support continued ATP production [23].

Following the S-deprivation paradigm of unicellular green algae, studies were performed in this work to probe for the effect of S-deprivation on cellular metabolism and H_2-production in purple photosynthetic bacteria. It was reasonably expected that, like in green microalgae, S-deprivation would prevent *de novo* biosynthesis of S-containing amino acids (cysteine and methionine), thereby inhibiting biosynthesis of new protein and cell growth. It was of interest to test whether purple bacteria would show a shift similar to that of green microalgae in terms of metabolism and catalysis, when challenged with sulfur starvation and in the face of abundant sources of carbon and electrons [16,24]. In this context, it has been shown that the nitrogenase enzyme is capable of evolving hydrogen under N-repressing conditions, presumably to serve as an electron sink and to maintain redox poise [25].

It is reported here that S-deprivation caused inhibition of nitrogenase activity, including N_2-fixation and H_2-production, and a concomitant enhancement in storage polymer accumulation. Physiological, biochemical, and molecular analyses were conducted to dissect and elucidate these phenomena, induced in purple photosynthetic bacteria upon sulfur-deprivation conditions.

2. Materials and methods

2.1. Organisms and growth media

Unless otherwise noted, *Rhodospirillum rubrum* UR2 (gift from Dr. Paul Ludden) was used in this study. Ormerod medium [26] was used for cell growth and H_2-production, with 16 mM Na-succinate as the organic carbon substrate and photosynthetic electron donor. The growth medium contained 3 mM Na-glutamate, as a nitrogen source, serving to enhance growth and hydrogen production without repressing the nitrogenase enzyme [27]. The growth medium was supplemented with 0.06 μM biotin [28]. Starter cultures were grown in supplemented minimal medium (SMN), containing 0.3% bacto-tryptose (Difco) and 0.3% bacto-yeast extract (Difco) supplemented to Ormerod medium [29]. Sulfur-deprivation medium was identical to the Ormerod growth medium except for a replacement of sulfate salts with their chloride equivalents. Where noted, some experiments were performed in parallel using *Rhodobacter sphaeroides* 2.4.1.(ATCC 17023) and *Rhodopseudomonas palustris* CGA009 (gift from Dr. Carolyn Harwood). In these cases, Ormerod medium (both S-replete and S-deplete) were supplemented with 3 μM thiamine, 8 μM nicotinic acid, and 0.016 μM biotin for *R. sphaeroides*, or 3 μM para-aminobenzoic acid for *R. palustris* [28].

2.2. Culture conditions

Starter cultures were inoculated with 500 μL frozen aliquots of purple bacterial strains into 20 mL screw-cap glass tubes containing SMN medium and grown with mixing by inversion every 12 h. Twenty four hours after photomorphogenesis occurred, 3 mL of these starter cultures were inoculated into flat Roux-type bottles containing 1 L Ormerod medium. Inoculated cultures were sealed with a three-port silicon stopper and placed in a temperature-controlled room at 24 °C on magnetic stir-plates. Irradiance from a combination of fluorescent and incandescent light bulbs was set at 60 W m^{-2}, as measured with a LI-COR 185B Radiometer equipped with a pyranometer sensor. Cultures were bubbled with Argon aseptically for 5 min through the long-needle port in the stopper while stirring. Sulfur-deprivation was performed by centrifugation of cultures at 5000*g* for 10 min (Beckman

J2-21M centrifuge with a JA-10 rotor), rinsing the pellet with 200 mL sulfur-deplete medium, centrifugation for another 10 min, and finally resuspension of the pelleted cells in 1 L sulfur-deplete medium. Control cultures were set up, originating from the same source culture, and were subjected to the same regimen but resuspended in sulfur-replete medium and not rinsed. Both sets of cell pellets endured an identical, simultaneous exposure to air during the centrifugation and resuspension steps; thus, immediately after resuspension, cultures were sealed and bubbled with Argon for 5 min to deaerate the headspace and medium and were subsequently placed under the same continuous light conditions and stirred magnetically for the duration of the experiment. For sulfur-replenishment experiments, 10 mL sterile 0.16 M $MgSO_4$ was added to both bottles after cessation of H_2 evolution by the control culture.

2.3. Physiological measurements

Hydrogen gas levels were recorded volumetrically by water displacement of a connected inverted 1 L graduated cylinder filled with water; purity of H_2 was ascertained to be greater than 85% by gas chromatography using an SRI 8610C Multiple Gas Analyzer equipped with a Molecular Sieve column and a TCD filament detector, using Ar as the carrier gas. Cell growth was determined by dry cell weight, bacteriochlorophyll (BChl) accumulation, and packed cell volume (PCV) measurements. Packed cell volume was quantitated using sealed glass tubes (macrohematocrits) and a swing-bucket centrifuge, as previously described [13]. Bacteriochlorophyll concentrations were measured by pigment extraction in 7:2 acetone:methanol solvent, followed by spectrophotometry at 775 nm in a Shimadzu UV160U spectrophotometer [30], in addition to estimating the absorbance at 887 nm *in vivo* as previously described [13]. Absorbance at 887 has been previously shown to scale linearly with the extracted concentration values. Protein was quantitated by the Lowry method using a Bio-Rad D_C Protein Assay kit (Bio-Rad, Hercules, CA, USA), with bovine serum albumin as the standard. Whole-cell nitrogenase activity was measured by ethylene production from acetylene at 30 °C in illuminated 1 ml culture samples as previously described [31]. Poly-β-hydroxybutyrate accumulation (PHB) was measured spectrophotometrically using the glass disk method [32]. Imaging of PHB granules was performed by staining 1 mL cultures with 20 μL of Nile Red solution (100 μg/mL in DMSO), incubation in the dark for 15 min, and imaging by fluorescence microscopy on a Zeiss Axioimager M1 fluorescence microscope using a 100× oil-immersion lens with DIC and also with a FITC filter with an excitation bandpass of 470–490 nm and an emission longpass of 505 nm. Micrographs were taken with a Qimaging micropublisher color camera and using IVision software (version 4.0.11).

2.4. Cell viability

Cell viability measurements were conducted with a LIVE/DEAD BacLight Bacterial Viability Kit (Molecular Probes, L13152). 2.5 μL propidium iodide solution (24 μM in water) was mixed with 0.5 μL Syto 9 solution (600 μM in DMSO) and 2 μL H_2O, which was subsequently mixed with 5 μL fresh sample and incubated in the dark for 15 min. Microscope slides were prepared by mixing 10 μL stained cells with warm molten 2% agarose onto a warmed slide and promptly applying the coverslip. Triplicate images (DIC, FITC fluorescence filter, and dsRed filter) were taken with a 20× oil-immersion lens using fluorescence imaging microscopy, as described above. The dsRed filter had an excitation bandpass of 520–560 nm and an emission longpass of 570 nm. A minimum of ten fields of view were counted from three slides each, from three independent replicate cultures each. Each field of view had from 30 to 150 cells, all of which were scored to be either ''live'' or ''dead''. Cells permeabilized with 70% isopropanol for 15 min and resuspended in 0.9% NaCl were used as a control, in addition to cells stained with each dye independently.

2.5. Aconitase activity

Aconitase activity was measured spectrophotometrically with the method described by Kennedy et al. [33], using anaerobic buffers and reagents throughout the sample preparation. Cell extracts were prepared from pellets of 10 mL of culture, resuspended with 225 μL sonication buffer (100 mM Tris–HCl (pH 7.5), 50 mM NaCl), treated with 25 μL lysozyme (5 mg/mL in buffer), and incubated 45 min on ice. 250 μl more buffer was added, and samples were sonicated 2–3 times with 1 min cycles at 4 °C. Extracts were spun at 20,000×g for 30 min in a tabletop Eppendorf centrifuge and the supernatant was injected into small anaerobic bottles. Aconitase activity assay was prepared using 10–25 μL extract plus 1 mL anaerobic isocitrate reagent (90 mM Tris–HCl, pH 8.0, 20 mM isocitrate). A_{240} was recorded every 30 s for 5 min and the slope of the curve was determined. Controls run with buffer lacking the isocitrate and, alternatively, lacking the extract showed no change in absorbance. Exposure of samples to air for 3 h caused a 25% decline in activity. An extinction coefficient of 3.6 $mM^{-1}\,cm^{-1}$ was used to calculate the activity of the extracts, with one Unit of enzyme required to produce 1 μmol *cis*-aconitate min^{-1}.

2.6. Western blotting

Samples for protein analysis were taken and immediately precipitated with trichloroacetic acid [34]. Protein pellets were then resuspended in water and subsequently solubilized 1:1 with a custom-made solubilization buffer (MMSB). MMSB was made as a 90% 2× stock, pH 6.8, containing 250 mM Tris, 4% SDS, and 20% glycerol, and a few grains of Bromophenol Red. Bromophenol Red was selected as a suitable pH indicator dye in order to bring TCA-precipitated samples back up to pH 6.8; Bromophenol Red was found to undergo a color change from yellow at pH 5.5 to amber at 6.3 to pale red at 6.5 to red at 6.8 to fuschia at 7.2, when present in MMSB. MMSB aliquots were mixed 9:1 with β-mercaptoethanol prior to use, and an appropriate amount of 1 N NaOH solution (2–8 μL) was added to the solubilized samples to turn the indicator dye to red again. Solubilized protein samples were then loaded onto a low-crosslinker polyacrylamide gel (containing 10% total acrylamide, 172:1 ratio of acrylamide to bisacrylamide) [35] and separated by SDS-PAGE [36]. Western blotting was performed on PVDF membranes with standard procedures.

Polyclonal antibodies, raised against the *R. rubrum* NifH and NifDK proteins were kindly provided by Dr. Paul Ludden [37].

2.7. RT-PCR

For RT-PCR experiments, total RNA was extracted from 1.5 mL of cell culture, using Trizol reagent (Invitrogen, Carlsbad, CA, USA) according to the manufacturer's instructions. Contaminating genomic DNA was removed using a TURBO DNA-free Kit (Ambion, Austin, TX, USA) and RNA purity was ascertained by confirming intact and sharp ribosomal bands after agarose gel electrophoresis. cDNA template was generated from 750 ng of total RNA using SuperScript II reverse transcriptase (Invitrogen, Carlsbad, CA, USA) with random hexamers, followed by amplification by PCR with 26, 35, and 26 cycles for the *nifH*, *amtB*, and *cysK* genes, respectively. Control reactions lacking the reverse transcriptase enzyme were run for each RNA sample and shown to be blank after 35 cycles. The following gene-specific primers were used:

1010F (5′–GAGAACAAGGCTCAGGAAATCTACATC–3′) and
1010R (5′–AATTCCATCAGCATCTCTTCCAGGTCTT–3′) for amplification of *nifH* cDNA,
1129F (5′-GAAGAAGACCCTGGGCTATGACGAC-3′) and
1129R (5′-ATGGCCAGATCAATGACCTTCAAGA-3′) for amplification of *amtB* cDNA
3794F (5′-ACTTCATCGATCAGGCTGACATC-3′) and
3794R (5′-CAGGAAATCTGGAACGATACCAAC-3′) for amplification of *cysK* cDNA.

3. Results

Research was performed to address the effect of sulfur-deprivation upon cellular metabolism and H_2-production in *R. rubrum*, as previously described in unicellular green algae [19,22,38]. In order to design such a S-deprivation process, the relationship between growth and H_2-production of *R. rubrum* UR2 was first defined in normal growth media. Fig. 1A shows biomass accumulation and H_2-production, measured as a function of growth time in batch culture. As indicated by the packed cell volume (PCV) and the bacteriocholorphyll quantitation, based on the absorbance of the culture at 887 nm, cell growth stopped at about 100 h after inoculation. Gas evolution (H_2) occurred concomitantly with growth (Fig. 1B); however, it continued well into the stationary phase, with maximal rates of hydrogen production at approximately 20 mL L^{-1} culture h^{-1}. In agreement with our previous work [13], average yields were 1600 ± 200 mL H_2 L^{-1} culture (57–74 mmol H_2 L^{-1} culture), with a supply of 16 mmol succinate L^{-1} culture. As calculated by Koku et al. [17], this indicates a molar substrate utilization efficiency ranging from 45 to 58%. In an attempt to improve this value, it was hypothesized that S-deprivation could serve to divert reducing equivalents away from growth and instead toward H_2-production. The point at which 700 mL gas was evolved was selected as an indicator for the phase of the culture during which the H_2 evolution rate was maximal, coinciding with late exponential growth phase (marked by an arrow in Fig. 1B); when H_2 collection reached this checkpoint, the cultures were harvested and resuspended according to the procedure described in the Methods section.

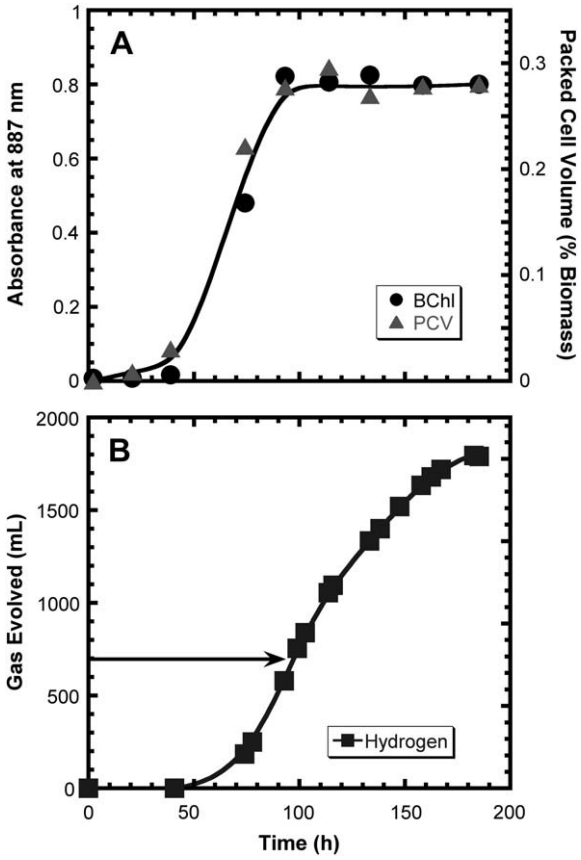

Fig. 1 – Cell growth and hydrogen production by *R. rubrum*. (A) Growth of *R. rubrum* as evidenced by accumulation of biomass (BChl absorbance at 887 nm and packed cell volume), commenced after a lag period of about 30 h following culture inoculation and reached stationary phase at about 100 h. (B) Hydrogen production commenced after a 50–60 h lag and stopped after about 220 h following inoculation. Hydrogen production thus continued for about 100 h beyond culture entrance to stationary phase. Arrow indicates the point-in-time and stage of growth chosen for culture resuspension in S-deplete or S-replete media. Such batch culture dynamics were observed across 19 independent replicate cultures for H_2-production, 9 replicates for BChl, and 11 replicates for PCV [13].

Upon resuspension of growing cultures in fresh growth medium, either containing or lacking sulfur nutrients, cellular growth was monitored from the bacteriochlorophyll (BChl) and protein content of the culture. The photosynthetic apparatus of *R. rubrum* lacks a peripheral BChl antenna for light intensity adaptations [39], and thus the BChl concentration scales linearly with biomass and protein content, and is a suitable indicator of cellular growth under photosynthetic growth conditions [13]. Fig. 2A shows that BChl accumulation resumed in the S-replete culture but halted abruptly in the S-deplete one. Similarly, protein accumulation in the S-replete culture resumed after resuspension, whereas in the S-deplete

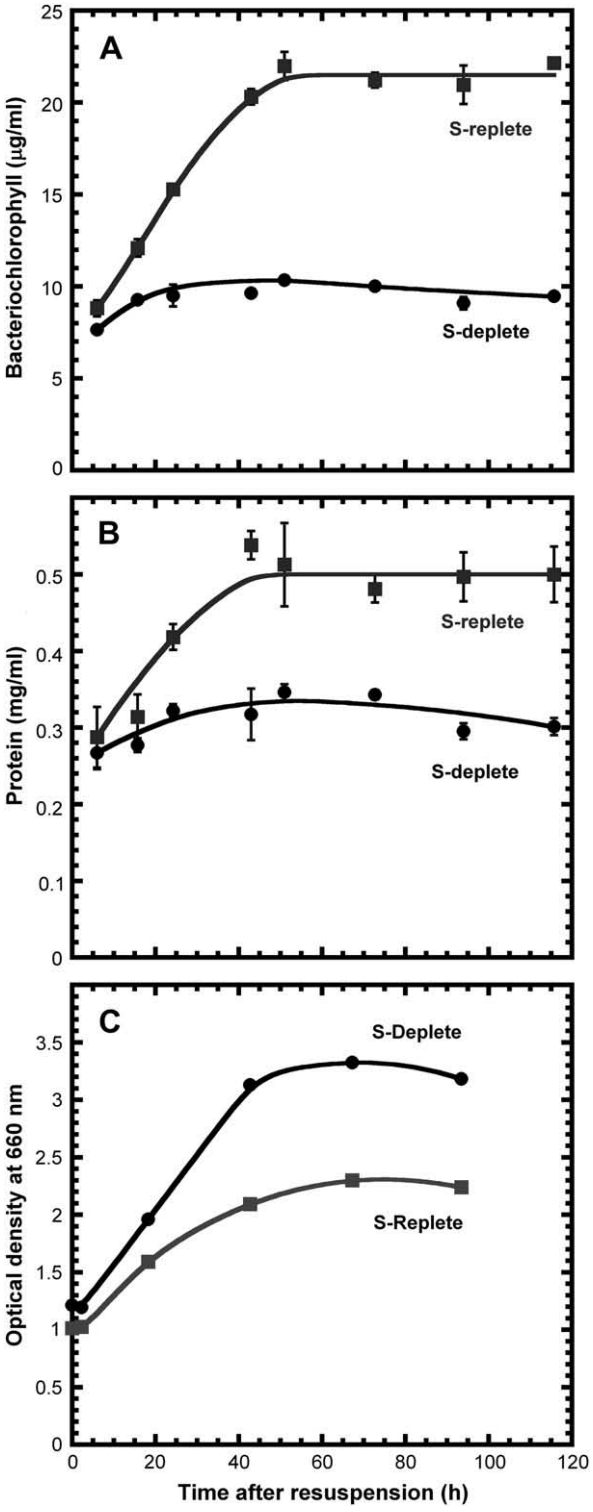

Fig. 2 – Effect of sulfur-deprivation on growth parameters. Growth of both S-deprived and S-replete cultures was investigated by estimation of BChl content using the *in vivo* absorbance at 887 nm (A) and of total cell protein using the Lowry method of protein quantitation (B). The nonspecific optical density of the cultures was also measured at 660 nm (C), representing a non-descript wavelength for the measurement of light scattering by the cells in the culture. Results in A and B are representative of the trend observed across 11 replicates for BChl and 6 replicates for protein. Results in C are representative of the phenomenon observed across 8 independent replicates.

culture protein ceased to accumulate after removal of S-nutrients (Fig. 2B, lower panel). Thus, it can be concluded from these measurements that removal of sulfur nutrients from the medium causes a cessation of cellular growth.

S-deplete cultures became turbid within 48 h of S-deprivation, remaining pink but cloudy, whereas the coloration of S-replete cultures continued to develop toward a bright, deep fuschia. As expected from the growth characteristics, observed in Fig. 2, the S-replete control cultures displayed an increase in the optical density at 660 nm (Fig. 2C). However, and in spite of a lack of growth (Fig. 2A,B), S-deplete cultures showed an even greater increase in 660 nm light scattering than that of the S-replete cultures (Fig. 2C). While optical density at 660 nm is traditionally used by microbiologists to indicate cellular growth, here it cannot be taken as such. Rather, it shows that S-deprivation has caused an increase in turbidity within the liquid cultures, resulting in greater light scattering. The cell physiology, biochemistry and regulation that underline these observations, and the effect of S-deprivation on H_2-production, were investigated in greater detail.

Upon resuspension of the cultures, hydrogen production resumed under S-replete conditions (Fig. 3A, S-replete) with a rate and yield that were about the same as in the control cultures (compare with Fig. 1B), continuing for approximately 100 h. However, contrary to expectation, H_2-production in the sulfur-deplete cultures halted within 24 h of resuspension (Fig. 3A, S-deplete). The *in vivo* activity of nitrogenase, the enzyme responsible for hydrogen production in purple photosynthetic bacteria, was assayed by acetylene reduction. Nitrogenase activity remained maximal in the S-replete cultures for approximately 50 h before it began to decline (Fig. 3B). Interestingly, nitrogenase activity declined promptly and exponentially with a halftime of ~15 h upon sulfur-deprivation, suggesting that cells lose the capacity to evolve hydrogen in response to this nutrient stress.

The reductase component of the nitrogenase enzyme complex, consisting of NifH homodimers, has been shown to be post-translationally modified in *R. rubrum* and other species in response to conditions such as darkness or N excess [40]. This process involves ADP-ribosylation of one of the two NifH polypeptides at a specific arginine residue, thereby inactivating the nitrogenase enzyme by preventing the reductase component from docking with the catalytic NifDK heterotetramer, halting electron flow between the two nitrogenase components [41]. ADP-ribosylation causes a slow-down in the SDS-PAGE electrophoretic mobility of the NifH subunit and thus leads to the appearance of two distinct NifH bands in Western blots. The ratio of the upper band to the lower band can be used to estimate the extent of post-translational inactivation of nitrogenase complexes, with equal intensity between the bands indicating complete inactivation [42].

Fig. 4A (left side) shows that indeed two distinct NifH bands develop quickly as a function of time in S-deprivation, indicating a shift in electrophoretic mobility in SDS-PAGE,

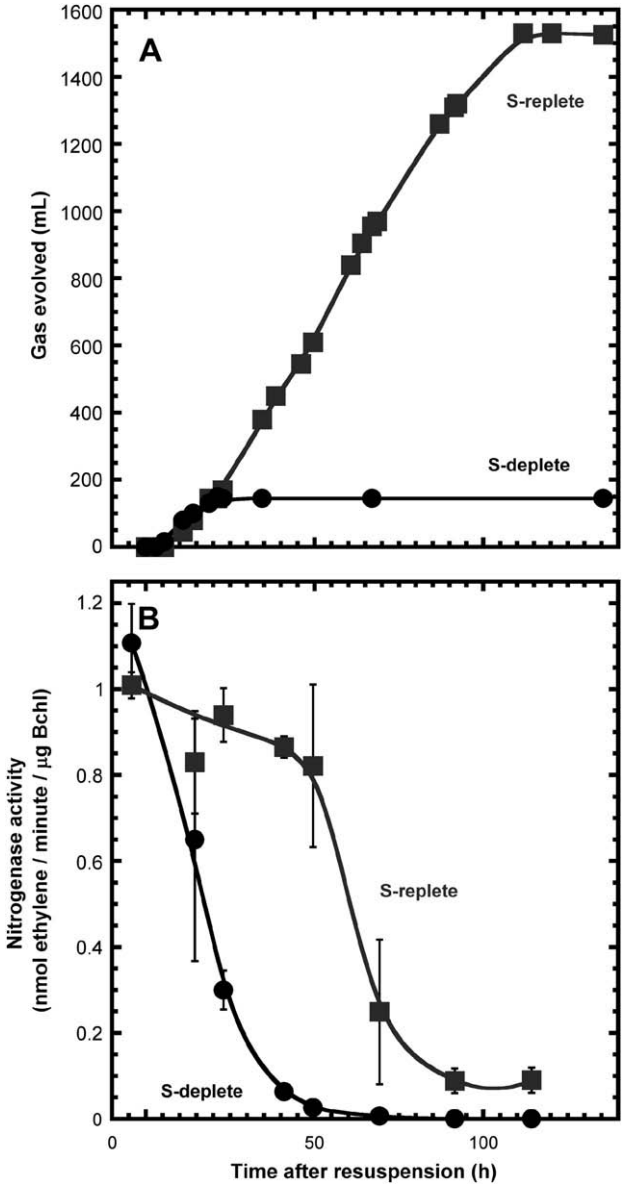

Fig. 3 – Hydrogen production and nitrogenase activity upon S-deprivation. (A) Hydrogen production was measured from the accumulation of gas collected in a gas trap. Collected gas was ascertained to be 85–98% pure H_2 by GC analysis. (B) Nitrogenase activity was measured by acetylene reduction of intact cells and normalized to BChl concentration. Results shown are representative of the trend observed across 20 independent replicate cultures for gas collection and 3 independent replicates for acetylene reduction.

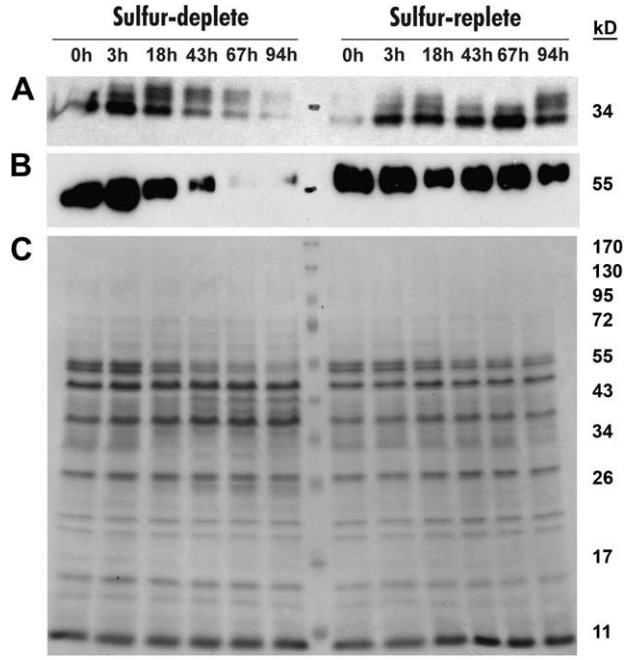

Fig. 4 – Nitrogenase protein levels as a function of time in S-deprivation. Western blots were performed on TCA-precipitated total protein from sulfur-deplete (left panels) and S-replete control cultures of *R. rubrum* (right panels). (A) Samples containing 0.01 μg BChl were blotted with specific polyclonal antibodies raised against the NifH protein. (B) Samples containing 0.2 μg BChl were blotted with specific polyclonal antibodies raised against the NifDK protein. (C) Protein samples containing 0.5 μg BChl were separated on SDS-PAGE and stained with Coomassie brilliant blue to view loading and protein profile. The phenomena depicted here were found to be consistent across twelve replicate western blots for each protein from four independent sets of cultures.

presumably due to ADP-ribosylation. Specifically, after 18 h of S-deprivation, approximately 50% of the NifH proteins showed a shift to slower electrophoretic mobility during SDS-PAGE, as evidenced by equal intensity of upper and lower bands in NifH Western blots (Fig. 4A, left side). However, in the replete cultures, the majority of the antibody intensity exists in the lower of the two NifH bands for most of the time-points (Fig. 4A, right side). Nevertheless, at the 94 h time-point of the S-replete control, a larger amount of intensity begins to appear in the upper band, suggesting significant ADP-ribosylation of NifH and inactivation of nitrogenase; this coincides with about the time when H_2 evolution stops (Fig. 3A) and cultures have progressed well into the stationary phase (Fig. 2). Moreover, the total amount of NifH protein diminished as a function of time in S-deprivation (Fig. 4A, left side), whereas NifH remained present in fairly constant amounts in the S-replete culture throughout the time course of this experiment (Fig. 4A, right side).

The abundance of the NifDK polypeptides, which comprise the catalytic component of nitrogenase, showed the same trend as the NifH, evidenced in Western blot analysis with specific anti-NifDK antibodies: the amount of the NifDK polypeptides declined with time under S-deprivation conditions (Fig. 4B, left side) but remained at a constant level in the S-replete culture throughout the time course of this experiment (Fig. 4B, right side). These results suggested that S-deprivation of *R. rubrum* might lead to degradation of the nitrogenase enzyme.

The nitrogenase enzyme contains many Fe–S centers, along with the requisite S-containing Cys residues that serve

as ligands to these cofactors. A question was raised as to whether degradation of the nitrogenase enzyme upon S-deprivation was associated with a global S-scavenging mechanism, designed to reallocate sulfur from abundant S-rich proteins toward functions that are essential for survival. To test this hypothesis, activity of aconitase, another enzyme containing Fe–S centers, was assayed in order to determine whether other Fe–S proteins were downregulated upon S-deprivation. In addition to its role in the citric acid cycle, the aconitase enzyme possesses a secondary function as a sensor of oxidative stress, due to the cytoplasmic exposure and lability of its Fe–S center [43]. However, Fig. 5 shows that aconitase activity remained fairly constant throughout both the S-deplete and S-replete conditions, with similar levels of activity. Thus, it appears that degradation and loss of activity of the nitrogenase is not a general problem of proteins containing Fe–S centers.

To investigate whether the cessation of hydrogen production was the result of transcriptional signaling, expression of the genes *nifH*, *amtB* (encoding for the ammonium channel), and *cysK* (encoding for the cysteine synthase) was investigated by RT-PCR as a function of time following cell resuspension in S-deplete or S-replete conditions. The transcriptional control of *nifH* is known to depend upon internal nitrogen pools [44] in addition to energy availability [45,46] and oxygen sensitivity. *amtB* transcription is likewise regulated by nitrogen availability [47] and can act as a sensor of ammonium concentration [48] and was thus used here as a control. The investigation of a *cysK* transcriptional response to S-deprivation served not only to determine whether a S-scavenging response exists in *R. rubrum*, as the case is in other microorganisms [49,50] but, moreover, as a positive control to denote the presence of cDNA in the late S-deprived samples.

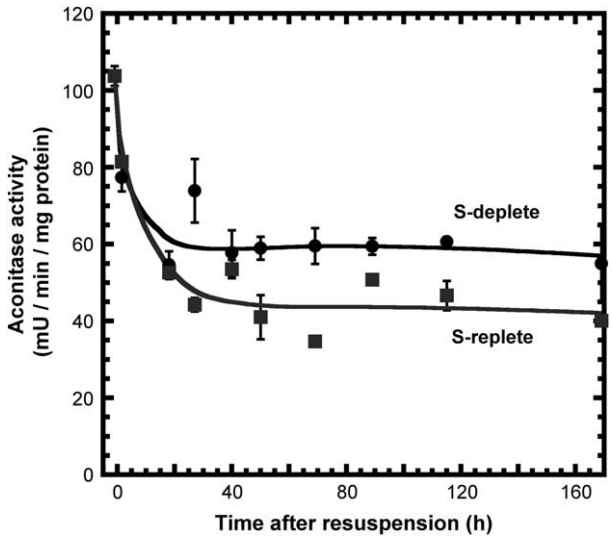

Fig. 5 – Aconitase activity as a function of time in S-deprivation. Anaerobically-prepared cell extracts were assayed for aconitase activity spectrophotometrically. Reproducibility of the results was tested via replicate cultures with two extracts at each time-point. For more details, please see Materials and methods.

Fig. 6A shows the RT-PCR analysis with primers specific for the *nifH* gene. Based on the levels of *nifH* mRNA, it is seen that the *nifH* gene is turned off completely within 24 h of S-deprivation, but remains on throughout the S-replete conditions. *amtB* follows the same pattern as *nifH*, albeit with somewhat slower kinetics (Fig. 6B), suggesting that both genes are being regulated by the S-deprivation condition. On the other hand, expression of *cysK* was induced substantially at 48 h after S-deprivation (Fig. 6C), proving the presence of template in late S-deprivation samples, and additionally demonstrating that cultures are transcriptionally active throughout S-deprivation. Fig. 7 provides a densitometric quantitation of the RT-PCR results shown in Fig. 6, further underlining the anti-parallel response of *nifH* and *amtB* from that of *cysK* upon S-deprivation.

As described above, the optical density of S-deprived cultures increased dramatically throughout S-deprivation (Fig. 2C) despite a lack of growth (Fig. 2). Additionally, the packed cell volume (PCV) of S-deprived cultures increased by about 3-fold within 100 h after resuspension in S-deplete medium (Fig. 8A, Total). Analysis revealed that the PCV due to purple cell matter in the culture nearly doubled within this period of time (Fig. 8A, Purple). This result is interpreted as a swelling of cell volume (see below) and not as cell proliferation, because of the cessation of protein and BChl accumulation (Fig. 2A,B). Additionally, a cell-free white polymer material was seen accumulating in the lower portion of the packed cell volume tube (Fig. 8B, ''P''). This material was denser than the biomass, and its substantial extracellular accumulation contributed to the large increase in turbidity and the overall increase in the packed cell volume (Fig. 8A, White). The results of polymer accumulation reported here were independently confirmed upon density equilibrium measurements of control and S-deprived *R. rubrum*, in which PHB accumulation resulted in an overall greater density of the biomass [51]. The white biomass occasionally appeared slightly pink, which is probably due to pigments released from cell lysis; see below for a discussion of this phenomenon. A further observation from the PCV measurements is the absence of the aerobic form of *R. rubrum*, which was previously shown to appear as colorless cells above the heavier purple photosynthetic biomass [7], suggesting that the cultures remained anaerobic throughout the experiment.

Cells were stained with the lipophilic-specific bioprobe Nile Red and subsequently examined with light and fluorescence microscopy (Fig. 9). The differential interference contrast images showed that S-deprived cells (Fig. 9A) were larger than S-replete cells (Fig. 9C) and appeared swollen. Moreover, the S-deprived cells, when examined by fluorescence microscopy, exhibited bright foci of Nile Red fluorescence throughout the cells (Fig. 9B), suggesting the presence of storage polymer granules. However, S-replete cultures barely exhibited any fluorescence at all (Fig. 9D). Based on these and previous findings [18,52], the white material seen in the PCV measurements (Fig. 8) is proposed to contain the lipophilic storage polymer, poly-β-hydroxybutyrate (PHB). PHB levels of the bulk culture were applied to glass disks, treated with hypochlorite, and quantitated spectrophotometrically upon conversion to crotonic acid. This analysis revealed a 3–4-fold increase in PHB accumulation in S-deplete samples, occurring within 12 h of

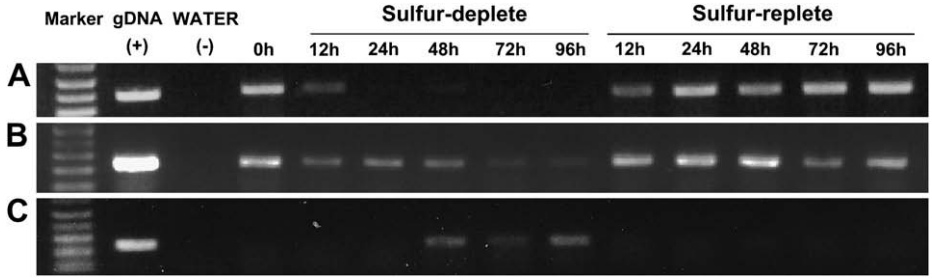

Fig. 6 – Transcriptional dynamics of *R. rubrum* genes under S-deprivation. Cycle-based RT-PCR was used to measure relative quantities of transcript from three selected genes. All experiments used purified genomic DNA (gDNA) as template for a positive control and water as a negative control. cDNA samples were ascertained to be free of contamination by running all samples through the same steps but lacking the reverse transcriptase enzyme (data not shown). (A) *nifH* was amplified for 26 cycles, (B) *amtB* was amplified for 35 cycles, and (C) *cysK* was amplified for 26 cycles.

S-deprivation (Fig. 10, S-deplete). A smaller increase in PHB content was also noted in the S-replete samples (Fig. 10, S-replete), occurring with slower kinetics, as the cells gradually approached the stationary phase. Thus, although it is clear that purple bacterial cultures deprived of sulfur nutrients redirect a substantial portion of their metabolism toward PHB accumulation, it is plausible that other metabolic pathways may also contribute to the observed increase in biomass production.

The presence of large amounts of extracellular PHB (Fig. 8) was peculiar in that secretion of this polymer has never been convincingly demonstrated. One explanation for this observation is that extracellular PHB may accumulate due to cell rupture upon swelling. Thus, cell viability was assayed to ascertain the extent of cellular death due to lysis. Cells were stained with a LIVE/DEAD cell viability kit, which stains live and dead cells differentially based on the integrity of the cell membrane to exclude an impermeable DNA-intercalating dye, propidium iodide. Upon thorough examination and counting of the differentially-emitting cells, it was estimated that approximately two-thirds ($69\% \pm 20$) of the cells in the S-deprived culture remained alive after 90 h of −S incubation. Nearly the entire population of cells in the S-replete culture ($94\% \pm 4$) excluded the propidium iodide dye, suggesting that the control cultures remained viable at 90 h after resuspension. Thus, it is likely that cell lysis of a substantial fraction of lysed cells in S-deprived cultures may contribute to the appearance of the white extracellular biomass.

In order to further investigate the cell physiology of this phenomenon, metabolic competence experiments were undertaken following 90 h of S-deprivation (Fig. 11). In these experiments, sulfate was supplemented to the medium in both S-replete and S-deplete cultures after the cessation of hydrogen production in the S-replete culture. Sulfur supplementation of S-replete cultures had no effect on hydrogen production (Fig. 11), or on growth, as measured by BChl and protein accumulation in the S-replete cultures (data not shown). However, upon S-supplementation to S-deprived cultures, H_2-production resumed with high rates, and hydrogen gas accumulated to the same yield that the S-replete culture had initially achieved.

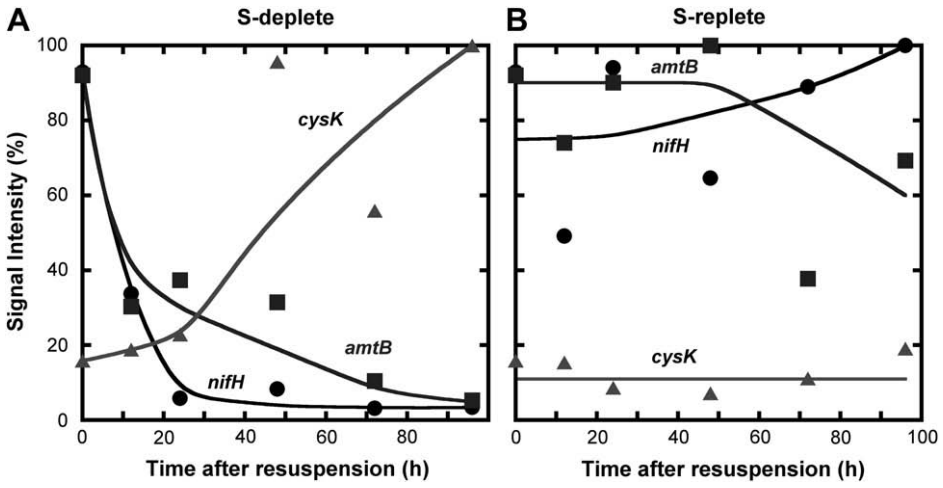

Fig. 7 – Densitometric analysis of *R. rubrum* transcriptional dynamics as a function of time in S-deprivation. Densitometry of the RT-PCR bands from Fig. 6is plotted as a function of time after resuspension of cells in S-deplete (A) or S-replete medium (B). Results were normalized to the maximal intensity for each gene product after subtraction of the average background intensity, with trend lines showing the proposed dynamics. The depicted phenomena were supported across experiments from four independent replicate cultures.

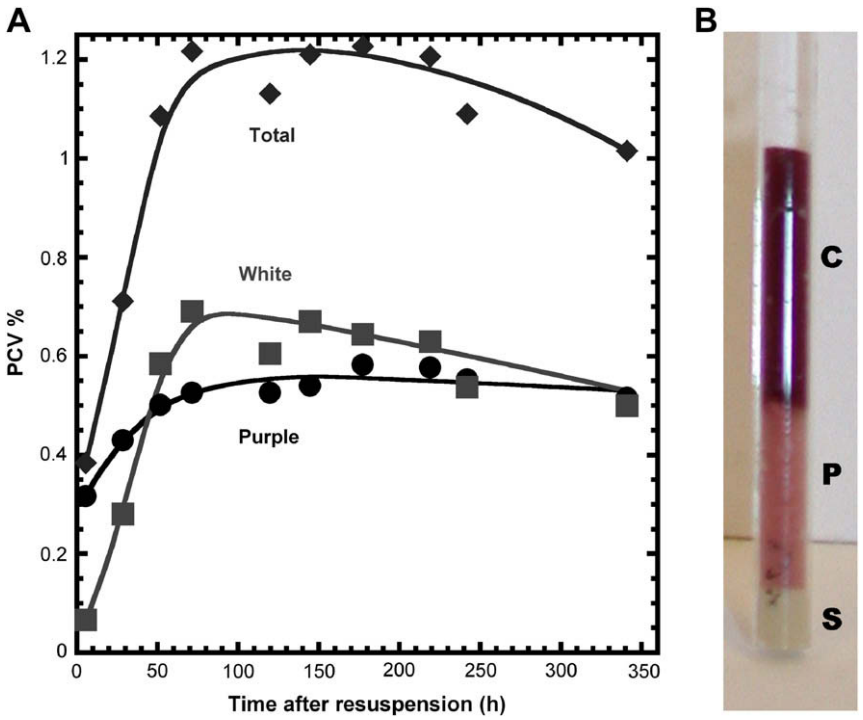

Fig. 8 – Packed Cell Volume (PCV) in S-deprived cultures. (A) PCV of purple cellular and white polymer biomass was quantitated, and expressed as a percent of the original volume of the culture. Results from one set of cultures is shown as a representative of six independent replicates, all displaying the same phenomenon. (B) Macrohematocrit tube showing the purple cellular packed biomass (upper layer, C) and the white polymer (middle layer, P) isolated from a culture after approximately 90 h of S-deprivation. The clay seal (lower layer, S), used to plug the hematocrit tube for centrifugation, can also be seen at the bottom.

Bacteriochlorophyll and protein levels also showed a similar stimulation upon S-supplementation to the S-deprived cultures (not shown). Thus, despite the potential of cellular lysis under S-deplete conditions, it seems that a large population of cells remained intact and metabolically competent, thus viable after 90 h of sulfur-deprivation, suggesting that this process of polymer-overproduction might be sustainable.

In order to examine the breadth of the findings in this work, S-deprivation was also conducted with cultures of *R. sphaeroides* and *R. palustris*. The cessation of growth and hydrogen production upon S-deprivation observed in *R. rubrum* also occurred with these disparate genera of purple photosynthetic bacteria. The S-deprived cultures of *R. sphaeroides* and *R. palustris* also became turbid, although further physiological analyses were not performed. Samples taken from *R. palustris*, as a function of time in S-deprivation, were used for Western Blotting, and showed a similar loss of NifH protein. NifDK proteins could not be detected using the antibodies raised specifically against the *R. rubrum* proteins. Nevertheless, these cursory results suggest that general aspects of the S-deprivation response in *R. rubrum* can be extended to include other purple photosynthetic bacteria.

4. Discussion

The present work was undertaken to explore the regulation of cellular metabolism and H_2-production upon sulfur-deprivation of *R. rubrum* cultures. The process of sulfur-deprivation was used as a physiological tool to shift cells from growth metabolism to a non-growing state (Fig. 2). It was found that the production of hydrogen ceased shortly after S-deprivation (Fig. 3A). This finding was elaborated, upon the observation of a rapid decline in activity of the nitrogenase (Fig. 3B), modification and subsequent degradation of the nitrogenase structural proteins (Fig. 4), and transcriptional down-regulation of the expression of the *nifH* gene (Fig. 6). Thus, it appears that all functions of the nitrogenase are promptly downregulated at multiple levels in response to S-deprivation, preventing any further production of hydrogen.

Cessation of nitrogenase activity and hydrogen production under S-deprivation conditions in purple photosynthetic bacteria is contrary to what was seen in unicellular green algae, where hydrogen production is substantially enhanced and sustained under S-deprivation conditions [19]. The basis of this difference is likely because of the physiological role of the respective hydrogen-evolving enzymes. In unicellular green algae, hydrogen is evolved by the [Fe]-hydrogenase, which is expressed only under anaerobic conditions. The latter conditions arise under S-deprivation in the green algae, so that the [Fe]-hydrogenase may serve as a ''vent'' for excess electrons, to prevent over-reduction of electron-transfer components in the chloroplast, and to sustain electron transport for the generation of ATP in both chloroplasts and mitochondria [23].

However, in purple photosynthetic bacteria, hydrogen is largely produced by the nitrogenase enzyme [5,53]. The obligate

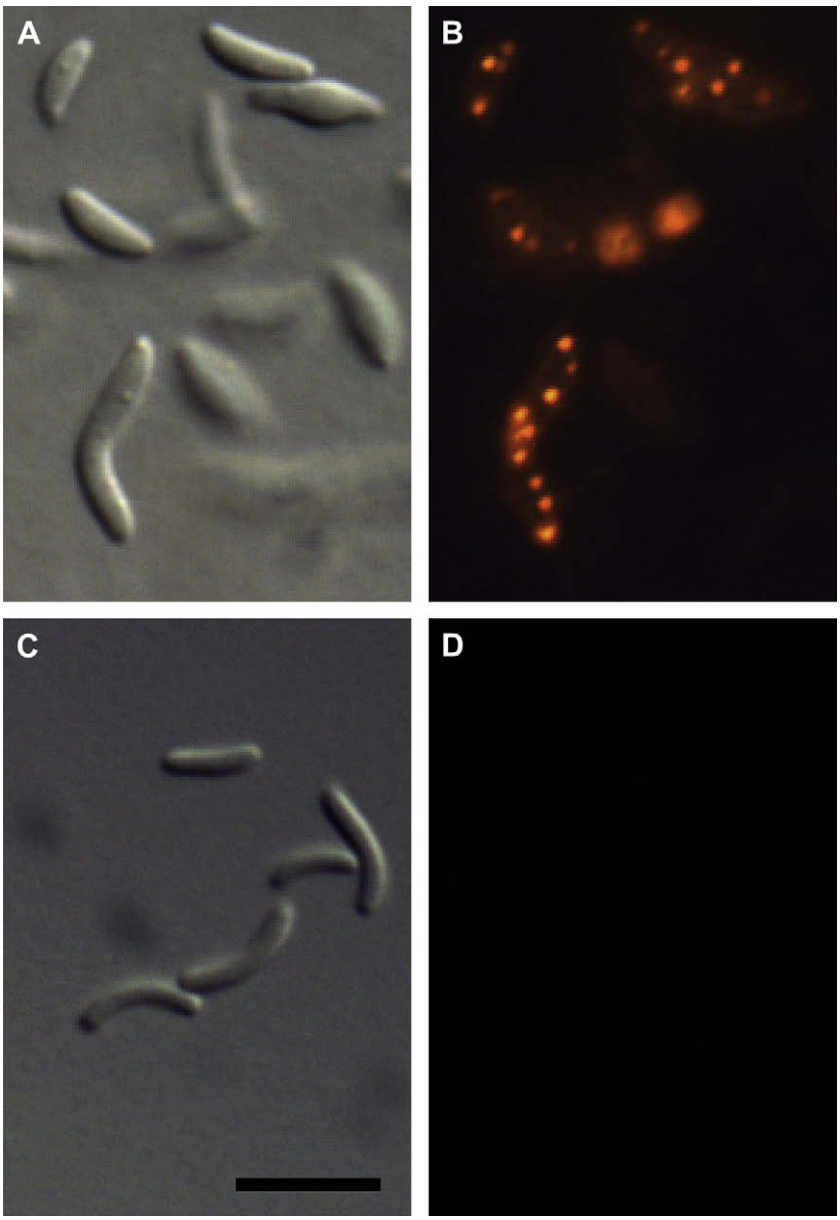

Fig. 9 – Morphological changes and accumulation of lipophilic compounds in *R. rubrum* under S-deprivation. Samples were taken at approximately 80 h following resuspension in S-deplete or S-replete media. All images were obtained at 40× with a Zeiss AxioImager M1 fluorescence microscope. (A, C) Differential Interference Contrast (DIC) images of S-deprived and S-replete cultures, respectively. (B, D) Fluorescence images (FITC filter) of S-deprived and S-replete cultures stained with 2 μg/mL Nile Red, respectively. The noted differences were observed across samples from at least four independent sets of cultures. Bar size is 10 μm.

proton-reducing function of this enzyme, resulting in hydrogen production [54], has indeed been shown to serve as a stress-release vent for excess reductant [25]. However, the primary function of the nitrogenase enzyme is the reduction of atmospheric N_2 for the production of ammonia, needed for cell growth. In *R. rubrum*, the nitrogenase enzyme is transcriptionally downregulated by N-excess conditions by the effect of P_{II} enzyme uridylylation status on the NifA transcriptional activator [44]. The activity of P_{II} transduces a signal based on the size of internal glutamine pools, reflecting the nitrogen status of the cell [55,56]. The *amtB* gene for the ammonium transport channel [48] is also regulated by nitrogen status and P_{II} activity, and this signal is transduced by the global regulator NtrC [47].

Because both *nifH* and *amtB* are downregulated under S-deprivation conditions (Figs. 6 and 7), and because of the cessation of growth under otherwise nutrient-rich conditions, it is hypothesized that nitrogenase, like *amtB*, is being down-regulated due to an excess of reduced nitrogen in the cells. Under such nitrogen excess, the primary function of the nitrogenase enzyme – production of NH_3 from N_2 – would not be necessary and might even be counterproductive as it would

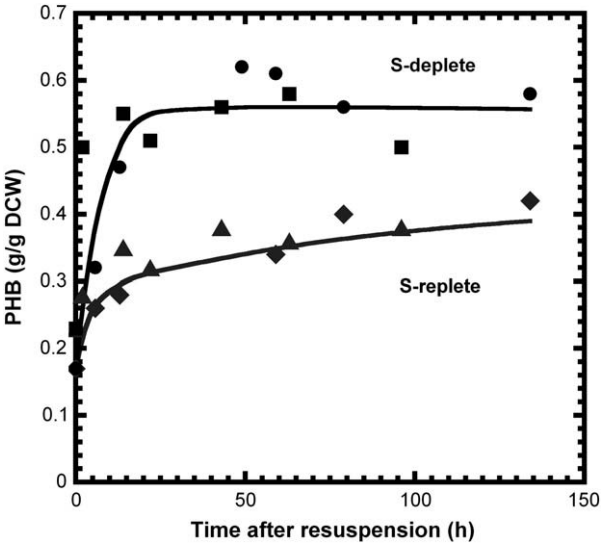

Fig. 10 – Poly-β-hydroxybutyrate (PHB) concentration as a function of time in sulfur-deprivation. PHB was quantitated spectrophotometrically, according to the method of Henrysson & McCarty [32], and expressed as a fraction of the total dry cell weight. Results for S-deplete (squares, circles) and S-replete (triangles and diamonds) cultures are shown. Samples from three independent cultures were tested in this experiment.

result in the accumulation of toxic NH_3. In *R. rubrum*, as well as several other diazotrophs, nitrogenase can be post-translationally modified by ADP-ribosylation via the DraT/DraG system [40], and this is reflected by the appearance of slower-migrating NifH protein bands in the SDS-PAGE/Western blot analysis of S-deprived cells (Fig. 4). It has been shown that the ADP-ribosylation activity is enhanced under nitrogen sufficiency conditions by membrane sequestration of the glycohydrolase ADP-ribose-removing enzyme, DraG [57]. This may represent the first step in the down-regulation [58] of the nitrogenase under S-deprivation conditions.

An interesting finding of this work was the production of large quantities of polymer material in response to S-deprivation (Fig. 8). A substantial portion of this productivity included PHB (Figs. 9 and 10), to the extent that cells swelled in volume (Fig. 9) and PHB accumulated both intra- and extracellularly (Figs. 8 and 9). Thus, it appears that, although reductant and energy cannot be redirected to enhance H_2-production by S-deprivation of purple photosynthetic bacteria, energy storage polymers such as PHB can be produced in large quantities by non-growing cells in a relatively short period of time (<24 h) after S-deprivation, even when succinate is the carbon substrate for growth. The partition of exogenously provided organic carbon substrate between PHB and glycogen in *R. rubrum* was not further investigated in this work, but is the subject of on-going research in this lab. Nevertheless, it can be concluded that in the absence of protein biosynthesis, imposed upon the cells by S-deprivation, cellular metabolism is effectively redirected toward storage polymer formation. Further elaboration of this method could potentially lead to a sustainable and commercially viable process of PHB production. Moreover, such polymers can serve as energy storage molecules that could be reversibly mobilized toward cell growth, and/or H_2-production, under the proper cell growth conditions.

It is of interest that substantial amounts of PHB, and possibly other cellular polymers, are found as cell-free material in the S-deprived cultures. Cell viability was determined to

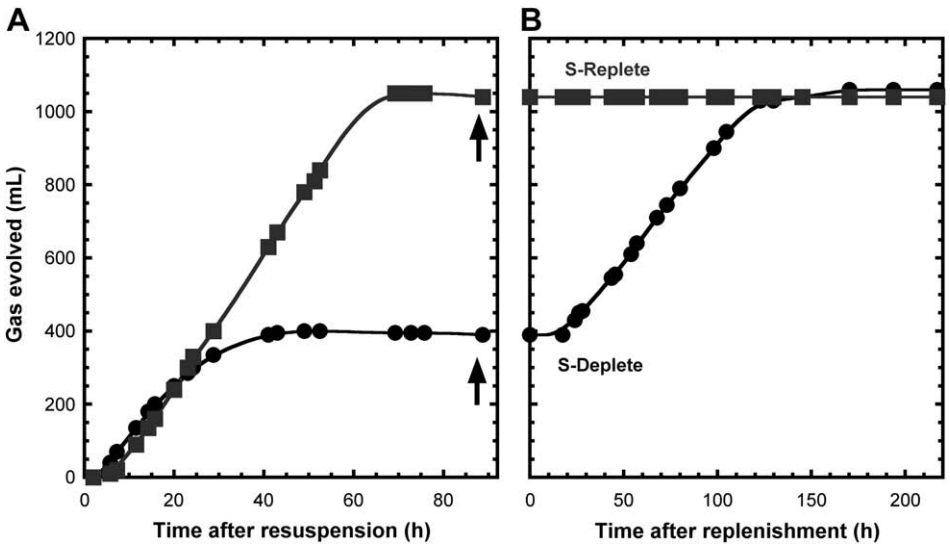

Fig. 11 – Recovery of H_2-production in S-deprived *R. rubrum* upon S-replenishment. H_2-production was measured in S-deprived cultures in comparison to control S-replete cultures (A, left panel, same conditions as Fig. 3A). However, 90 h after resuspension, both cultures were replenished with sulfur by injecting 1.6 mmol $MgSO_4$ (indicated by arrows) in order to investigate the metabolic competence of the cells and remaining H_2-production capability of the respective cultures (B, right panel). The depicted phenomena were reproducibly observed in two independent experiments with *R. rubrum*, and further reproduced with a culture of *R. sphaeroides* (data not shown).

be slightly diminished 90 h after removal of S-nutrients (Fig. 11), suggesting that a fraction of the PHB-swollen cells may have ruptured. The reason for and mechanism of the appearance of extracellular PHB could be due to cell lysis, secretion, or a combination of both. Several studies have cited extracellular release of PHB from cells [59–61]; however, none have tested to see the extent to which cells remained viable. According to one model by Stubbe & Tian [62], PHB granule formation may be initiated in the inner membrane of bacterial cells. Thus, a plausible explanation for the large amount of extracellular PHB may be due to excretion from rapid synthesis of PHB induced upon S-deprivation. If cells indeed excrete PHB while remaining viable, this would present an interesting opportunity for the industrial production of biodegradable plastics, permitting product separation from the biomass without any prior harvesting of the cells [63]. Of interest in this respect is the observation that *R. rubrum* possesses high levels of PHB depolymerase activity [64]. Several bacteria have been shown to possess extracellular PHB depolymerase activity [65], and indeed a periplasmic depolymerase has been discovered in *R. rubrum* [66]. Accordingly, it is plausible that jettisoning of excess PHB may occur under high rates of PHB biosynthesis, and serve as an extracellular auxiliary carbon and energy storage that can later be utilized during prolonged starvation.

Cessation of growth upon sulfur-deprivation (Fig. 2) has been observed in other systems [19]. Without sulfur nutrients in the growth medium, cells will deplete their internal pools of the S-containing amino acids, cysteine and methionine. A specific sulfur-starvation response to these depletions has been demonstrated in several bacteria, involving nutrient scavenging and homeostatic responses [49,67,68]. Although *cysK* is induced by S-deprivation (Figs. 6 and 7), suggesting such a response, the sustained activity of the Fe–S-containing aconitase enzyme (Fig. 5), and the minimal loss of cell viability (Fig. 11), imply that the method of S-deprivation does not cause irreparable damage to *R. rubrum* over the period of time studied.

The determination of cell growth in this research demonstrated an important pitfall in physiological growth analyses. Two commonly employed measurements of growth – light-scattering via optical density and packed cell volume – would suggest that cultures had grown during S-deprivation (Figs. 2C and 8). This, however, was contrary to the result of measurements from protein and bacteriochlorophyll accumulation (Fig. 2). The increase in turbidity (Fig. 2C) and in PCV (Fig. 8) in S-deplete cultures, therefore, should not be taken to indicate cellular growth, as is often used in physiological studies. On the contrary, cultures became turbid because of increased PHB content (Fig. 8) and PCV increased due to cellular swelling (Fig. 9). This demonstrates the need for multiple orthogonal measurements to assess growth of microbial cultures subjected to new external conditions, and illustrates the common inadequacy of optical density approaches to growth measurements.

The findings here suggest that industrial systems may be envisioned whereby PHB would serve as an alternative product of photosynthesis in purple bacteria, similar to that proposed by Vincenzini et al. [18]. A shift in metabolism between H_2-production and PHB production can be governed by the availability of S-nutrients. As shown in Fig. 11, this alteration of productivity is reversible, in that replenishment of S-nutrients to S-deprived cultures shifts the metabolism back toward growth and H_2-production. Cycles of limiting S-nutrients may be applied in a semi-continuous fed-batch process, similar to that described previously [13].

5. Concluding remarks

This research investigated alterations in hydrogen production and polymer accumulation upon S-deprivation in purple photosynthetic bacteria. Under physiological growth conditions, cells produce H_2 as a result of nitrogenase catalysis. Under nutrient-stress conditions in the absence of growth, when light and organic carbon substrate are present, substantial amounts of PHB accumulate. This shift in cellular metabolism, driven by photosynthesis, might find application in an alternating system of H_2 and polymer production.

Acknowledgements

Graduate student support by a "Berkeley Fellowship" to Matthew R Melnicki and postdoctoral fellowship support from "The Scientific and Technological Research Council of Turkey (TUBITAK)" to Ela Eroğlu are gratefully acknowledged. Thanks are due to Leonardo Curatti for his help with acetylene reduction and aconitase activity assays, and to Paul Ludden and Caroline Harwood for their provision of purple bacterial strains and antibodies.

REFERENCES

[1] Drews G. Forty-five years of developmental biology of photosynthetic bacteria. Photosynth Res 1996;48(3):325–52.
[2] Fuller RC. Polyesters and photosynthetic bacteria: from lipid cellular inclusions to microbial thermoplastics. In: Blankenship RE, Madigan MT, Bauer CE, editors. Anoxygenic photosynthetic bacteria. Netherlands: Kluwer Academic Press; 1995. p. 1245–56.
[3] Prince RC, Kheshgi HS. The photobiological production of hydrogen: potential efficiency and effectiveness as a renewable fuel. Crit Rev Microbiol 2005;31(1):19–31.
[4] Burris RH. Nitrogenases. J Biol Chem 1991;266(15):9339–42.
[5] Vignais PM, Colbeau A, Willison JC, Jouanneau Y. Hydrogenase, nitrogenase, and hydrogen metabolism in the photosynthetic bacteria. Adv Microb Physiol 1985;26:155–234.
[6] Melis A. Photosynthetic H_2 metabolism in *Chlamydomonas reinhardtii* (unicellular green algae). Planta 2007;226(5): 1075–86.
[7] Melis A, Melnicki MR. Integrated biological hydrogen production. Int J Hydrogen Energy 2006;31(11):1563–73.
[8] Nath K, Das D. Improvement of fermentative hydrogen production: various approaches. Appl Microbiol Biotechnol 2004;65(5):520–9.
[9] Basak N, Das D. The prospect of purple non-sulfur (PNS) photosynthetic bacteria for hydrogen production: the present state of the art. World J Microbiol Biotechnol 2007; 23(1):31–42.

[10] Das D, Veziroglu TN. Advances in biological hydrogen production processes. Int J Hydrogen Energy 2008;33(21): 6046–57.
[11] Eroğlu I, Aslan K, Gunduz U, Yucel M, Turker L. Substrate consumption rates for hydrogen production by *Rhodobacter sphaeroides* in a column photobioreactor. J Biotechnol 1999; 70(1–3):103–13.
[12] Rocha JS, Barbosa MJ, Wijffels RH. Hydrogen production by photosynthetic bacteria: culture media, yields and efficiencies. In: Miyake J, Matsunaga T, San Pietro A, editors. Biohydrogen II: an approach to environmentally acceptable technology. London: Pergamon; 2001. p. 3–32.
[13] Melnicki MR, Bianchi L, De Philippis R, Melis A. Hydrogen production during stationary phase in purple photosynthetic bacteria. Int J Hydrogen Energy 2008;33(22):6525–34.
[14] Eroglu E, Gunduz U, Yucel M, Turker L, Eroglu I. Photobiological hydrogen production by using olive mill wastewater as a sole substrate source. Int J Hydrogen Energy 2004;29(2):163–71.
[15] Zhu HG, Suzuki T, Tsygankov AA, Asada Y, Miyake J. Hydrogen production from tofu wastewater by *Rhodobacter sphaeroides* immobilized in agar gels. Int J Hydrogen Energy 1999;24(4):305–10.
[16] Rey FE, Heiniger EK, Harwood CS. Redirection of metabolism for biological hydrogen production. Appl Environ Microbiol 2007;73(5):1665–71.
[17] Koku H, Eroglu I, Gunduz U, Yucel M, Turker L. Aspects of the metabolism of hydrogen production by *Rhodobacter sphaeroides*. Int J Hydrogen Energy 2002;27:1315–29.
[18] Vincenzini M, Marchini A, Ena A, De Philippis R. H_2 and poly-β-hydroxybutyrate, two alternative chemicals from purple non sulfur bacteria. Biotechnol Lett 1997;19(8):759–62.
[19] Melis A, Zhang L, Forestier M, Ghirardi ML, Seibert M. Sustained photobiological hydrogen gas production upon reversible inactivation of oxygen evolution in the green alga *Chlamydomonas reinhardtii*. Plant Physiol 2000;122(1):127–35.
[20] Ghirardi ML, Zhang L, Lee JW, Flynn T, Seibert M, Greenbaum E, et al. Microalgae: a green source of renewable H_2. Trends Biotechnol 2000;18(12):506–11.
[21] Kredich NM. Biosynthesis of cysteine. In: Neidhart NC, Curtiss R, Ingraham JL, editors. *Escherichia coli* and *Salmonella*: cellular and molecular biology. Washington, DC: ASM Press; 1996. p. 514–27.
[22] Zhang L, Happe T, Melis A. Biochemical and morphological characterization of sulfur-deprived and H_2-producing *Chlamydomonas reinhardtii* (green alga). Planta 2002;214(4): 552–61.
[23] Melis A, Happe T. Hydrogen production. Green algae as a source of energy. Plant Physiol 2001;127(3):740–8.
[24] Zurrer H, Bachofen R. Hydrogen production by the photosynthetic bacterium *Rhodospirillum rubrum*. Appl Environ Microbiol 1979;37(5):789–93.
[25] Joshi HM, Tabita FR. A global two component signal transduction system that integrates the control of photosynthesis, carbon dioxide assimilation, and nitrogen fixation. Proc Natl Acad Sci USA 1996;93(25):14515–20.
[26] Ormerod JG, Ormerod KS, Gest H. Light-dependent utilization of organic compounds and photoproduction of molecular hydrogen by photosynthetic bacteria; relationships with nitrogen metabolism. Arch Biochem Biophys 1961;94(3): 449–63.
[27] Gest H, Kamen MD. Studies on the metabolism of photosynthetic bacteria. IV. Photochemical production of molecular hydrogen by growing cultures of photosynthetic bacteria. J Bacteriol 1949;58(2):239–45.
[28] Hutner SH. Organic growth essentials of the aerobic nonsulfur photosynthetic bacteria. J Bacteriol 1946;52(2): 213–21.
[29] Fitzmaurice WP, Roberts GP. Artificial DNA-mediated genetic transformation of the photosynthetic nitrogen-fixing bacterium *Rhodospirillum rubrum*. Arch Microbiol 1991;156(2): 142–4.
[30] Cohen-Bazire G, Sistrom WR, Stanier RY. Kinetic studies of pigment synthesis by non-sulfur purple bacteria. J Cell Comp Physiol 1957;49(1):25–68.
[31] Stewart WDP, Fitzgerald GP, Burris RH. In situ studies on N_2 fixation using the acetylene reduction technique. Proc Natl Acad Sci USA 1967;58(5):2071–8.
[32] Henrysson T, McCarty PL. Influence of the endogenous storage lipid poly-ß-hydroxybutyrate on the reducing power availability during cometabolism of trichloroethylene and naphthalene by resting methanotrophic mixed cultures. Appl Environ Microbiol 1993;59(5):1602–6.
[33] Kennedy MC, Emptage MH, Dreyer JL, Beinert H. The role of iron in the activation–inactivation of aconitase. J Biol Chem 1983;258(18):11098–105.
[34] Zhang Y, Burris RH, Ludden PW, Roberts GP. Posttranslational regulation of nitrogenase activity by anaerobiosis and ammonium in *Azospirillum brasilense*. J Bacteriol 1993;175(21):6781–8.
[35] Kanemoto RH, Ludden PW. Effect of ammonia, darkness, and phenazine methosulfate on whole-cell nitrogenase activity and Fe protein modification in *Rhodospirillum rubrum*. J Bacteriol 1984;158(2):713–20.
[36] Laemmli UK. Cleavage of structural proteins during the assembly of the head of bacteriophage T4. Nature 1970; 227(5259):680–5.
[37] Ludden PW, Preston GG, Dowling TE. Comparison of active and inactive forms of iron protein from *Rhodospirillum rubrum*. Biochem J 1982;203(3):663–8.
[38] Kruse O, Rupprecht J, Mussgnug JH, Dismukes GC, Hankamer B. Photosynthesis: a blueprint for solar energy capture and biohydrogen production technologies. Photochem Photobiol Sci 2005;4(12):957–70.
[39] Addlesee HA, Hunter CN. *Rhodospirillum rubrum* possesses a variant of the *bchP* gene, encoding geranylgeranyl-bacteriopheophytin reductase. J Bacteriol 2002;184(6): 1578–86.
[40] Halbleib CM, Ludden PW. Regulation of biological nitrogen fixation. J Nutr 2000;130(5):1081–4.
[41] Liang JH, Nielsen GM, Lies DP, Burris RH, Roberts GP, Ludden PW. Mutations in the *draT* and *draG* genes of *Rhodospirillum rubrum* result in loss of regulation of nitrogenase by reversible ADP-ribosylation. J Bacteriol 1991;173(21):6903–9.
[42] Preston GG, Ludden PW. Change in subunit composition of the iron protein of nitrogenase from *Rhodospirillum rubrum* during activation and inactivation of iron protein. Biochem J 1982;205(3):489–94.
[43] Beinert H, Kennedy MC, Stout CD. Aconitase as iron–sulfur protein, enzyme, and iron-regulatory protein. Chem Rev 1996;96(7):2335–73.
[44] Zou X, Zhu Y, Pohlmann EL, Li J, Zhang Y, Roberts GP. Identification and functional characterization of NifA variants that are independent of GlnB activation in the photosynthetic bacterium *Rhodospirillum rubrum*. Microbiology 2008;154(9):2689–99.
[45] Norén A, Soliman A, Nordlund S. The role of NAD^+ as a signal during nitrogenase switch-off in *Rhodospirillum rubrum*. Biochem J 1997;322(Pt 3):829–32.
[46] Zhang Y, Wolfe DM, Pohlmann EL, Conrad MC, Roberts GP. Effect of AmtB homologues on the post-translational regulation of nitrogenase activity in response to ammonium and energy signals in *Rhodospirillum rubrum*. Microbiology 2006;152(7):2075–89.
[47] Zimmer DP, Soupene E, Lee HL, Wendisch VF, Khodursky AB, Peter BJ, et al. Nitrogen regulatory protein C-controlled genes

of *Escherichia coli*: scavenging as a defense against nitrogen limitation. Proc Natl Acad Sci USA 2000;97(26):14674–9.
[48] Javelle A, Severi E, Thornton J, Merrick M. Ammonium sensing in *Escherichia coli*. Role of the ammonium transporter AmtB and AmtB–GlnK complex formation. J Biol Chem 2004; 279(10):8530–8.
[49] Gyaneshwar P, Paliy O, McAuliffe J, Popham DL, Jordan MI, Kustu S. Sulfur and nitrogen limitation in *Escherichia coli* K-12: specific homeostatic responses. J Bacteriol 2005;187(3):1074–90.
[50] Chen HC, Newton AJ, Melis A. Role of SulP, a nuclear-encoded chloroplast sulfate permease, in sulfate transport and H_2 evolution in *Chlamydomonas reinhardtii*. Photosynth Res 2005;84(1–3):289–96.
[51] Eroglu E, Melis A. ''Density equilibrium'' method for the quantitative and rapid in situ determination of lipid, hydrocarbon, or biopolymer content in microorganisms. Biotechnol Bioeng 2009;102(5):1406–15.
[52] De Philippis R, Ena A, Guastini M, Sili C, Vincenzini M. Factors affecting poly-β-hydroxybutyrate accumulation in cyanobacteria and in purple non-sulfur bacteria. FEMS Microbiol Rev 1992;103(2–4):187–94.
[53] Igarashi RY, Seefeldt LC. Nitrogen fixation: the mechanism of the Mo-dependent nitrogenase. Crit Rev Biochem Mol Biol 2003;38(4):351–84.
[54] Simpson FB, Burris RH. A nitrogen pressure of 50 atmospheres does not prevent evolution of hydrogen by nitrogenase. Science 1984;224(4653):1095–7.
[55] Arcondéguy T, Jack R, Merrick M. P_{II} signal transduction proteins, pivotal players in microbial nitrogen control. Microbiol Mol Biol Rev 2001;65(1):80–105.
[56] Ikeda TP, Shauger AE, Kustu S. *Salmonella typhimurium* apparently perceives external nitrogen limitation as internal glutamine limitation. J Mol Biol 1996;259(4):589–607.
[57] Wang H, Franke CC, Nordlund S, Noren A. Reversible membrane association of dinitrogenase reductase activating glycohydrolase in the regulation of nitrogenase activity in *Rhodospirillum rubrum*; dependence on GlnJ and AmtB1. FEMS Microbiol Lett 2005;253(2):273–9.
[58] Kranz RG, Cullen PJ. Regulation of nitrogen fixation genes. In: Blankenship RE, Madigan MT, Bauer CE, editors. Anoxygenic photosynthetic bacteria. Netherlands: Kluwer Academic Press; 1995. p. 1191–208.
[59] Çetin D, Gündüz U, Eroğlu I, Yücel M, Türker L. Poly-ß-hydroxybutyrate accumulation and releasing by hydrogen producing bacteria, *Rhodobacter sphaeroides* O.U.001. A transmission electron microscopic study. Afr J Biotechnol 2006;5(22):2069–72.
[60] Page WJ, Sherburne R, D'Elia L, Graham LL. Poly (ß-hydroxybutyrate) extrusion from pleomorphic cells of *Azotobacter vinelandii* UWD. Can J Microbiol 1995;41: 22–31.
[61] Resch S, Gruber K, Wanner G, Slater S, Dennis D, Lubitz W. Aqueous release and purification of poly (ß-hydroxybutyrate) from *Escherichia coli*. J Biotechnol 1998; 65(2–3):173–82.
[62] Stubbe J, Tian J. Polyhydroxyalkanoate (PHA) homeostasis: the role of the PHA synthase. Nat Prod Rep 2003;20(5):445–57.
[63] Hejazi MA, Wijffels RH. Milking of microalgae. Trends Biotechnol 2004;22(4):189–94.
[64] Merrick JM, Doudoroff M. Depolymerization of poly-ß-hydroxybutyrate by an intracellular enzyme system. J Bacteriol 1964;88(1):60–71.
[65] Jendrossek D. Microbial degradation of polyesters: a review on extracellular poly(hydroxyalkanoic acid) depolymerases. Polymer Degrad Stabil 1998;59(1–3):317–25.
[66] Handrick R, Reinhardt S, Kimmig P, Jendrossek D. The ''intracellular'' poly(3-hydroxybutyrate) (PHB) depolymerase of *Rhodospirillum rubrum* is a periplasm-located protein with specificity for native PHB and with structural similarity to extracellular PHB depolymerases. J Bacteriol 2004;186: 7243–53.
[67] Koch DJ, Ruckert C, Albersmeier A, Huser AT, Tauch A, Puhler A, et al. The transcriptional regulator SsuR activates expression of the *Corynebacterium glutamicum* sulphonate utilization genes in the absence of sulphate. Mol Microbiol 2005;58(2):480–94.
[68] Tralau T, Vuilleumier S, Thibault C, Campbell BJ, Hart CA, Kertesz MA. Transcriptomic analysis of the sulfate starvation response of *Pseudomonas aeruginosa*. J Bacteriol 2007;189(19): 6743–50.